Published in final edited form as:
Bone. 2010 July ; 47(1): 41–48. doi:10.1016/j.bone.2010.03.008.

The Effects of Axial Displacement on Fracture Callus Morphology and MSC Homing Depend on the Timing of Application

Aaron S. Weaver[1,2], **Yu-Ping Su**[1,3], **Dana L. Begun**[1], **Joshua D. Miller**[1], **Andrea I. Alford**[1], and **Steven A. Goldstein**[1]

[1] University of Michigan, Orthopaedic Research Laboratory, Ann Arbor, MI

[2] National Aeronautics and Space Administration, Glenn Research Center, Cleveland, OH

[3] National Yang-Ming University, School of Medicine, Department of Surgery, Taipei, Taiwan

Abstract

The local mechanical environment and the availability of mesenchymal stem cells (MSCs) have both been shown to be important factors in bone fracture healing. This study was designed to investigate how the timing of an applied axial displacement across a healing fracture affects callus properties as well as the migration of systemically introduced MSCs. Bilateral osteotomies were created in male, Sprague-Dawley rats. Exogenous MSCs were injected via the tail vein, and a controlled micro-motion was applied to one defect starting 0, 3, 10, or 24 days after surgery. The results showed that fractures stimulated 10 days after surgery had more mineral, less cartilage, and greater mechanical properties at 48 days than other groups. Populations of MSCs were found in osteotomies 48 days after surgery, with the exception of the group that was stimulated 10 days after surgery. These results demonstrate that the timing of mechanical stimulation affects the physical properties of the callus and the migration of MSCs to the fracture site.

Keywords

mesenchymal stem cells; mechanical strain; fracture healing

Introduction

Normal fracture healing is a process unique from typical wound healing in that there is a complete reconstitution of the bone without the formation of scar tissue. Secondary fracture healing occurs through both intramembranous and endochondral bone formation, mimicking embryonic bone development. This healing occurs in non-discrete stages until lamellar bone bridges the fracture gap to completely restore mechanical stability. The immediate response to fracture is the formation of a hematoma and inflammation. This response serves to initially provide stabilization between the two bone ends and to initiate signaling cascades vital to the healing process. After the hematoma has formed, precursor cells invade to form new blood vessels, fibroblasts, and other supporting cells that form granulation tissue between the fractured ends. Macrophages and other cells derive from this tissue act to remove the original

Steven Goldstein, University of Michigan, Orthopaedic Research Laboratories, Department of Orthopaedic Surgery, 109 Zina Pitcher Pl, Room 2001, Ann Arbor, MI 48109.

hematoma. Osteoclasts then begin to resorb the damaged and necrotic bone ends, and osteoprogenitors from the periosteum proliferate. Through intramembranous ossification, these osteoprogenitors form woven bone creating a hard callus on the periphery. At the same time, cells from the periosteum and surrounding tissues begin to form cartilage within the granulated scaffold, this cartilage matrix mineralizes, and bone forms through endochondral ossification. Finally, the woven bone that now constitutes the fracture callus is remodeled to return the bone to its original state. [1–4]

Published data demonstrates that the local mechanical environment contributes significantly to the progress of fracture repair. Small, controlled displacements can increase bone formation [5], callus size [6,7], and tensile strength [6]. Moreover, fractures subjected to cyclic compression demonstrate higher torque and energy to failure, higher torsional stiffness, more advanced tissue differentiation, and more complete bony bridging than when rigidly fixed [8, 9].

The availability of mesenchymal stem cells (MSCs) at the fracture site is also an important factor in healing. It may be advantageous to use MSCs to augment fracture repair, since they are involved in every aspect of bone regeneration [10]. Exogenous MSCs have been used to repair critical sized, segmental bone defects in animal models [10–13], and they have been shown to increase bone mineral content and growth velocity in children with severe osteogenesis imperfecta [14,15]. MSCs have also been used to treat defects in tissues other than bone including traumatic brain injury [16,17], infarcted myocardium [18], and cerebral ischemia [19,20], demonstrating their diverse promise for tissue repair.

Considering the influence of both progenitor cell availability and the mechanical environment on healing progression, their interplay on callus properties and cell migration to the site of repair may be critical to the quality of healing. The purpose of this study was to evaluate the temporal effect of a controlled mechanical environment on fracture repair in concert with systemic cell delivery. Specifically, this study was designed to investigate how the timing of an applied axial displacement following a femoral osteotomy affects callus morphology and the mechanical properties of the healing fracture site. We also evaluated the migration of systemically introduced, exogenous MSCs to determine if the timing of the applied displacement has an effect on the homing of these cells to the fracture site.

Methods

Animal Surgery and Mechanical Stimulation

One hundred five, six-month-old, male, Sprague-Dawley rats underwent a 2mm segmental osteotomy in the mid-diaphysis of each femur (Figure 1). Briefly, after a 1cm exposure and elevation of the soft tissues, four 0.062-inch diameter threaded pins were placed through predrilled holes made in the diaphysis using a specialized guide. A two-piece external fixator with locking plate was then affixed to the pins, and an osteotomy was created with an oscillating saw under constant saline irrigation. After surgery, all of the animals were allowed normal ambulation with the fixators locked, except when they were undergoing mechanical stimulation. All experimental procedures were approved by the University of Michigan Committee on Use and Care of Animals.

Axial mechanical stimulation was performed with a system that provides controlled axial motion with displacement monitored by a linear variable differential transformer (LVDT). The rats were placed in a sling so that the fixator could be properly aligned, and the locking plate was removed once it was secured in the loading device (Figure 1). Axial displacement was applied to one randomly chosen limb, while the other femur served as a contralateral control. The timing of the stimulation was chosen to roughly correspond with the stages of secondary

fracture healing. Mechanical stimulation occurred for five consecutive days beginning at 0, 3, 10, or 24 days postoperatively (groups A through D respectively) at a magnitude of ±8% strain (±0.16 mm) and a rate of 0.313 Hz for 510 loading cycles. An additional group, group DNC (n=6), served as a no cell control and paralleled group D. Rats were euthanized 10, 24, or 48 days post-operatively (Table 1).

MSC Culture and Injection

Bone marrow was harvested from the femora and ulnae of 2- to 4-month-old green fluorescent protein (GFP) transgenic rats and the cells were cultured in Dulbecco's Modified Eagle Medium (DMEM, Invitrogen, Carlsbad, CA) containing 10% fetal bovine serum (Fisher Scientific, Waltham, MA) and 1% antibiotic/antimycotic (Invitrogen) at 37°C, in 5% CO_2, and 95% humidity. In order to maintain the influence of non-adherent cells [21], half of the total volume of culture medium was replaced every three to four days. After 12–14 days, the cells were released from the cell culture plate using 0.25% trypsin containing 1 mM EDTA, and the cells were replated at 700,000 cells per 10cm culture dish. After reaching confluence, the cells were passaged again. Twenty-four hours later, the growth medium was removed and replaced with a serum free defined medium consisting of a 60%/40% mixture of DMEM/MCDB201 (Invitrogen/Sigma-Aldrich, St. Louis, MO) containing 1% antibiotic/antimycotic (Invitrogen), 1% linoleic acid bovine serum albumin (Sigma), 0.01% platelet-derived growth factor-β (Cell Signaling Technology, Danvers, MA), 0.001% basic fibroblast growth factor (Cell Signaling), and 0.05% insulin (Sigma). (Cell culture technique adapted from [22].) In preparation for injection, cells were trypsinized and resuspended in 1ml PBS at 1 million cells per ml per injection. Injections were performed via the tail vein immediately before the first application of axial displacement, with the exception of group DNC, which received no cells.

Microcomputed Tomography

Immediately after sacrifice, both femora were excised and the surrounding soft tissue was removed without disturbing the callus around the fracture site. Bones were scanned via *ex-vivo* micro-CT (GE Healthcare Pre-Clinical Imaging, London, ON) at a voxel size of 18μm. A region of interest (ROI) was created encompassing the 2mm osteotomy site and any remaining cortical bone was subtracted from the region. The lateral borders of the ROI were defined by visible mineralization on the outermost boundary of the callus. A threshold of 1200 was chosen for the gray scale value to define bone voxels for all specimens. Callus volume, bone volume, bone mineral content (BMC), bone mineral density (BMD), tissue mineral content (TMC), tissue mineral density (TMD), and bone volume fraction (BVF) were recorded for each osteotomy.

Histology

After sacrifice, femurs from five animals per group were placed in 10% neutral buffered formalin for three days. The specimens were then placed into 70% ethanol until they were processed. Specimens were embedded in poly(methyl methacrylate) (PMMA) and cut into 5μm thick, longitudinal sections at five different levels spaced 200–300μm apart through the thickness of the bone. Sections were mounted and then either processed for immunohistochemistry as outlined below, or stained using safranin-O to identify cartilage. Fast green was used as a nuclear counter stain. Six images per section were captured at 2.5 times magnification (Axiovert 200M, Carl Zeiss, Oberkochen, Germany) and stitched together using Photoshop (Adobe, San Jose, CA). One section per level was analyzed for a total of five sections per specimen. Each image was cropped to a height of 2mm to correspond to the size of the original osteotomy, and a boundary was drawn encompassing the callus periphery to quantify the callus area per section. Areas of cartilage and bone were quantified through color thresholding in Photoshop. Bone and cartilage areas were normalized to the callus area for each

section, and the values for the five sections per specimen were averaged to arrive at a cartilage/callus area and bone/callus area for each bone.

Immunohistochemistry (IHC)

Slides were deacrylized in a 1:1 mixture of xylene and chloroform for 30 minutes, rehydrated through a series of alcohol baths, and decalcified in 8% formic acid for ten minutes. Next, the sections were incubated in a proteinase K solution for 30 minutes at 37°C. The proteinase K solution was rinsed by a five-minute water bath, and then the endogenous peroxidases were quenched with a 10:1 mixture of methanol and 30% H_2O_2 for 30 minutes. The sections were flushed twice with distilled water and then twice covered with PBS containing 0.1% Triton X-100 (TPBS) for five minutes each. Non-specific sites were blocked using a solution of 10% normal goat serum (Vector Laboratories, Burlingame, CA), in 0.02% TPBS containing 1.5% bovine serum albumin (BSA, Sigma). Then, sections were incubated overnight at 4°C with a rabbit anti-rat GFP antibody (Fisher Scientific) diluted 1:1000 in 0.02% TPBS containing 1.5% BSA. The slides were then rinsed with PBS and incubated with biotinylated goat anti-rabbit immunoglobin-G (Vector Laboratories) diluted 1:500 in 0.02% TPBS containing 1.5% BSA. After washing with PBS, the slides were incubated with Vectastain Elite ABC reagent (Vector Laboratories) for 30 minutes at room temperature. Then, they were washed with PBS, incubated with stable DAB (Invitrogen) for two minutes, rinsed gently with tap water, counterstained with fast green, and cover slipped.

Torsion Testing

The femurs from the remaining animals were tested to failure in a custom designed torsion fixture. The bone ends were secured in aluminum pots with molten bismuth that was then allowed to cool. The pots were fastened on each side of the testing apparatus, and the bones were hydrated with lactated ringers solution. The locking plate of the fixator was then removed, and the bones were tested to failure at a rate of 0.5 deg/sec. A custom MATLAB (Mathworks, Natick, MA) script was used to determine the stiffness, ultimate failure torque, failure twist, and energy to failure.

Statistical Analysis

All data are expressed as means ± one standard error. A two-way, repeated measures ANOVA was run for all of the data using SAS (Cary, NC). Effects of treatment (mechanically stimulated versus control) and timing of displacement initiation, as well as the interaction between treatment and timing were analyzed. A Tukey-Kramer post-hoc adjustment was used to correct for multiple comparisons. Values were considered statistically different at $p \leq 0.05$.

For IHC analysis, three of the five levels per bone were used for a qualitative analysis. The levels chosen (levels one, three, and five) represent a symmetric view of the whole callus. Cells were viewed in the marrow within the medullary canal and peripheral callus. Due to difficulty in cell counting, a scoring system was developed. A score of zero corresponds to no cells present, a score of one represents 1–10 cells, and a score of two signifies that 11 or more cells were present in the marrow.

Results

Micro-CT analysis of callus mineralization suggests that the timing of mechanical stimulation had a significant impact on repair. Twenty-four days after surgery, fracture gaps that were stimulated on day three have less mineral than those stimulated on either day zero or day ten (Figure 2), and this difference reached significance between groups B (stimulation day 3) and C (stimulation day 10). Forty-eight days after surgery, there was more mineral in the defects displaced ten days post surgery (group C48) compared to those from the group displaced three

days post surgery (group B48) (Figure 3). There is also a trend toward a higher TMD in group C48 than in B48 (data not shown).

Histology shows that in fractures stimulated ten days after surgery, increased mineral content is associated with a significant decrease in cartilage (Figure 4). Similarly, the loaded limbs in group C48 have significantly less cartilage than their contralateral controls ($p=0.045$), while the loaded limbs in group A48 have more cartilage than their contralateral controls ($p=0.037$). There is also a difference in cartilage area between limbs stimulated at day ten and limbs that were stimulated at day zero ($p=0.031$) or day three ($p=0.015$) (Figure 5).

Figure 6 shows that stimulation starting at day three (group B10) induced more cartilage formation by day ten compared to stimulation immediately after surgery (group A10). The data also show that the control limbs in the B10 group have a larger cartilage area than the controls from group A10 suggesting that locally applied loads might exert systemic effects. In animals euthanized on day 48, there is a significantly larger percentage of bone in the fracture gaps as measured by histology on both the loaded and control sides for the animals stimulated starting on day ten (group C48) than for any other group (Figure 7). There is also more bone in the control defect of group C48 than for D48. The torsion data shows that bones from animals displaced on day ten are more stiff and stronger in torsion than bones from any other groups (Figure 8). The controls from that group are also significantly stiffer and have a higher failure torque than the control bones from animals stimulated on day 24.

IHC shows that even though there are a small number of exogenous MSCs present throughout the healing process, the largest population of cells does not appear until 48 days after surgery. At that time, MSCs are detected in large populations throughout the marrow in the medullary canal and the marrow spaces within the periosteal callus (Figure 9). This is true for all of the groups euthanized on day 48 except for the group stimulated ten days post-op (group C). In group C48, very few stained cells were found in relation to the other groups euthanized on day 48 (A48, B48, and D48). It also appears that stimulation increases the number of cells in the fractured limb, as the scores for the stimulated limbs were higher than the control limbs at most time points (Table 2).

To look at the effect that the cells may have on healing, a group in which exogenous cells were not injected was compared via micro-CT and mechanical testing in torsion to the group D48. The group without cells had a higher bone volume, BMC, BMD, TMC, and BVF than the group with injected cells. Stiffness and torque to failure were also higher in the group without exogenous cells as compared to the group that had cells delivered via the tail vein (Figure 10).

Discussion

Published data from multiple laboratories suggest that mechanical stimulation can modulate the fracture healing process. Here, we have extended these observations by demonstrating that the application of a defined axial displacement has a definitive effect on fracture healing. Specifically, our data show that the timing of the stimulus is an important factor in determining the progression of callus morphology and mechanical properties. Differences in healing due to displacement can be seen as early as ten days after fracture. By day 24, the group that was displaced three days after surgery (group B24) had a decrease in mineralization on the displaced side in comparison to the other groups. Forty-eight days after surgery, the group stimulated ten days post-op (group C48) had an elevated mineral content and almost no cartilage remaining on the stimulated side, while all the other groups still displayed a significant amount of cartilage.

The observation that the application of displacement soon after surgery decreased mineralization and mechanical properties compared to the animals that were stimulated starting

on day ten suggests that axial mechanical stimulation may not be beneficial during the initial response to fracture. Vascular supply is an important factor in determining the success of healing, and it may be necessary to allow neovascularization to progress at the site of repair before mechanical load is applied [23,24]. Early motion at the fracture site causes the capillaries needed to support osseous tissues to constantly rupture, which promotes fibrocartilage formation since it requires less vascularization [25]. Therefore, it may be beneficial to the overall healing outcome to delay initiation of loading until new vessels have had a chance to form [26].

Our results also suggest that it may be beneficial to start fracture stimulation after the inflammatory stage, when some soft tissue has had a chance to form. After the initial inflammatory response, cells that may be responsive to load, such as chondrocytes, have an opportunity to populate the fracture site. A potential beneficial response to chondrocyte loading in fracture healing has been shown previously. Scaffolds seeded with chondrocytes that were implanted in the femora of rabbits and then compressively loaded had a higher bone volume fraction than the unloaded controls [27], showing that the application of a stimulus to a chondrocyte population may encourage bone formation at the site of repair.

Our results also suggest that a local mechanical stimulus can influence callus properties in the contralateral fracture site, and that the timing of load influences the magnitude of these systemic effects. At day ten, the animals loaded three days post-operatively (group B10) exhibited significantly more cartilage as a whole (loaded and control combined) than those loaded immediately after surgery. At day 48, the group loaded ten days post-op (group C48) had a significantly higher bone to callus ratio, stiffness, and failure torque as a whole when compared to all other groups suggesting that, in this group, the applied stimulus increased bone formation and mechanical properties in both the loaded and control defects. This is consistent with findings that skeletal injury elicits an osteogenic response at distant sites [28]. Einhorn and colleagues demonstrated markedly increased mineral apposition rates in both tibiae following surgically-induced injury to the right femur [29]. Transverse loading of the knee has also been shown to accelerate healing in defects in the tibial diaphysis [30].

This systemic response may be due to the release of soluble factors into circulation as a result of the applied stimulus. Matrix-metalloproteinase-1 (MMP-1), basic fibroblast growth factor (bFGF), transforming growth factor β1 (TGF-β1), IGF binding protein 3 (IGFBP-3), and human growth hormone (hGH) have all been shown to be increased in the sera of patients undergoing distraction osteogenesis [31]. Sera from fracture patients and patients undergoing distraction osteogenesis have also been shown to promote proliferation of osteoblasts, and TGF-β and IGF-I were shown to be important in those processes [32,33]. Increased proliferation of osteoblasts was only induced by sera of patients after the fractures had some time to heal, and proliferation was actually decreased when sera from the first week of healing was used [33]. Vascular endothelial growth factor (VEGF), which is important for the formation of new blood vessels, has been shown to be elevated in the muscles surrounding a distraction site as well as the muscles surrounding the contralateral control site [34]. It is feasible that the controlled displacement at the experimental site could increase the concentration of growth factors critical to fracture healing [35] in the bloodstream that would then influence the progression of repair in the contralateral osteotomy.

The presence of GFP positive cells confirmed that donor MSCs are able to migrate to the femora, where, in most cases, they establish a population in the marrow by day 48. This is consistent with other studies that have found exogenous MSCs in the bone marrow for long periods after a systemic injection [36], and they do not appear in large numbers in the first few weeks after delivery [37]. Our results also suggest that the presence of exogenous cells can have a deleterious effect on the fracture healing process. The animals that were stimulated and

received cells on day 24 exhibited less mineralization and lower mechanical properties in torsion than animals from the same group that underwent displacement but did not receive cells. Taken together, our histology and micro-CT results indicate a trend for a deleterious effect of exogenous MSC in all groups except the one stimulated starting on day 10 (Group C48). This group had the lowest number of exogenous MSCs present around the fracture site and also had the highest mineral content, as well as evidence of accelerated fracture healing. While this result appears to support the suggestion that the exogenous MSC are deleterious to repair process, an alternative explanation cannot be excluded. Stimulation at 10 days may have enhanced MSC migration and promoted differentiation onto osteoblast progenitors and increased bone formation. Subsequently, they may have been removed through remodeling, resulting in their absence in the marrow and tissue at 48 days.

The original strategy for the GFP model to track exogenous cells was to image the cells through fluorescence microscopy. To facilitate this, the specimens were embedded in PMMA instead of paraffin to reduce background fluorescence, but even with this precaution, the fluorescence from the surrounding mineral was too large to be able to detect individual GFP-positive cells. Due to this complication, the IHC procedure outlined in the methods was developed to visualize the GFP-positive cells. Sectioning the PMMA blocks for the IHC procedure proved to be difficult and led to the scoring system for cell counting. While an actual cell count or a cell count per unit area would have been ideal, we believe that the scoring system developed accurately represents the number of GFP-positive cells detected.

Given the extent of work in the literature on the influence of introduced MSC on bone repair, the intent of this study was to focus on the local response to a mechanical stimulus with respect to both callus morphology and MSC homing. As such, the unstimulated, contralateral control limb was the main control group for these experiments. During early examination of the results, it became clear that several other interesting trends, including the systemic response to the stimulation and the deleterious effect of the injected MSCs, might be occurring. As a result, we had the ability to add one no-cell control group (group DNC) within the context and timing of the study. Clearly, our results raise questions about the role of exogenous MSC and additional testing should be performed to fully examine their influence on the repair process.

In summary, our data indicate that the timing of application of a controlled axial displacement determines the effects of mechanical stimulation on callus morphology and mechanical properties. Stimulation early in the repair process was not beneficial to fracture healing, but when the displacement was applied after the inflammatory phase it increased mineralization, accelerated callus remodeling, and increased torsional mechanical properties in comparison to other groups. This effect was seen in both the experimental and the contralateral control limbs, indicating that there may be a systemic effect of the applied stimulus. Similarly, our data suggest that the relationship between introduction of exogenous MSCs and fracture healing progression may also depend on timing. Mechanical stimulation, when applied after the initial healing stages, seemed to prevent these cells from engrafting in the marrow and also improved healing in comparison to the other groups. In addition, cell injections had a deleterious effect on fracture healing in animals that had cells delivered later in the healing process (day 24). These findings help to clarify the role of the timing of mechanical manipulation of fractures, and may help provide guidance for continuing studies focused on developing therapies for enhancing fracture repair.

Acknowledgments

We would like to thank Kathy Sweet, Bonnie Nolan, Charles Roehm, Dennis Kayner, Jaclynn Kreider, John Baker, Rochele Taylor, Michael Paschke, Stephanie A. Goldstein, Ralph Zade, David Lee, Srikanth Volvalou, and Eric Lee for their enormous contributions to this work. The study was funded by grants from the Department of Defense and the National Institutes of Health (AR51504).

Reference List

1. Day, SM.; Ostrum, RF.; Chao, EYS.; Rubin, CT.; Aro, HT.; Einhorn, TA. Bone Injury, Regeneration, and Repair. In: Buckwalter, JA., editor. Orthopaedic Basic Science: American Academy of Orthopaedic Surgeons. 2000. p. 371-99.
2. Einhorn TA. The cell and molecular biology of fracture healing. Clin Orthop Relat R Clin Orthop Relat R 1998:S7–S21.
3. Frost HM. The biology of fracture healing - An overview for clinicians. Part I. Clin Orthop Relat R Clin Orthop Relat R 1989:283–93.
4. McKibbin B. Biology of fracture healing in long bones. Journal of Bone and Joint Surgery-British Volume 1978;60:150–62. [PubMed: 350882]
5. Yamaji T, Ando K, Wolf S, Augat P, Claes L. The effect of micromovement on callus formation. Journal of Orthopaedic Science 2001;6:571–5. [PubMed: 11793181]
6. Claes LE, Wilke HJ, Augat P, Rubenacker S, Margevicius KJ. Effect of dynamization on gap healing of diaphyseal fractures under external fixation. Clinical Biomechanics 1995;10:227–34. [PubMed: 11415558]
7. Claes LE, Heigele CA, Neidlinger-Wilke C, Kaspar D, Seidl W, Margevicius KJ, Augat P. Effects of mechanical factors on the fracture healing process. Clin Orthop Relat R Clin Orthop Relat R 1998:S132–S147.
8. Goodship AE, Kenwright J. The influence of induced micromovement upon the healing of experimental tibial fractures. Journal of Bone and Joint Surgery-British Volume 1985;67:650–5. [PubMed: 4030869]
9. Wolf JW, White AA, Panjabi MM, Southwick WO. Comparison of cyclic loading versus constant compression in the treatment of long-bone fractures in rabbits. Journal of Bone and Joint Surgery-American Volume 1981;63:805–10.
10. Kraus KH, Kirker-Head C. Mesenchymal stem cells and bone regeneration. Vet Surg 2006;35:232–42. [PubMed: 16635002]
11. Arinzeh TL, Peter SJ, Archambault MP, van den Bos C, Gordon S, Kraus K, Smith A, Kadiyala S. Allogeneic mesenchymal stem cells regenerate bone in a critical-sized canine segmental defect. J Bone Joint Surg Am 2003;85-A:1927–35. [PubMed: 14563800]
12. Kon E, Muraglia A, Corsi A, Bianco P, Marcacci M, Martin I, Boyde A, Ruspantini I, Chistolini P, Rocca M, Giardino R, Cancedda R, Quarto R. Autologous bone marrow stromal cells loaded onto porous hydroxyapatite ceramic accelerate bone repair in critical-size defects of sheep long bones. J Biomed Mater Res 2000;49:328–37. [PubMed: 10602065]
13. Petite H, Viateau V, Bensaid W, Meunier A, de Pollak C, Bourguignon M, Oudina K, Sedel L, Guillemin G. Tissue-engineered bone regeneration. Nat Biotechnol 2000;18:959–63. [PubMed: 10973216]
14. Horwitz EM, Prockop DJ, Fitzpatrick LA, Koo WW, Gordon PL, Neel M, Sussman M, Orchard P, Marx JC, Pyeritz RE, Brenner MK. Transplantability and therapeutic effects of bone marrow-derived mesenchymal cells in children with osteogenesis imperfecta. Nat Med 1999;5:309–13. [PubMed: 10086387]
15. Horwitz EM, Gordon PL, Koo WK, Marx JC, Neel MD, McNall RY, Muul L, Hofmann T. Isolated allogeneic bone marrow-derived mesenchymal cells engraft and stimulate growth in children with osteogenesis imperfecta: Implications for cell therapy of bone. Proc Natl Acad Sci U S A 2002;99:8932–7. [PubMed: 12084934]
16. Lu D, Mahmood A, Wang L, Li Y, Lu M, Chopp M. Adult bone marrow stromal cells administered intravenously to rats after traumatic brain injury migrate into brain and improve neurological outcome. Neuroreport 2001;12:559–63. [PubMed: 11234763]
17. Mahmood A, Lu D, Wang L, Li Y, Lu M, Chopp M. Treatment of traumatic brain injury in female rats with intravenous administration of bone marrow stromal cells. Neurosurgery 2001;49:1196–203. [PubMed: 11846913]
18. Orlic D, Kajstura J, Chimenti S, Jakoniuk I, Anderson SM, Li B, Pickel J, McKay R, Nadal-Ginard B, Bodine DM, Leri A, Anversa P. Bone marrow cells regenerate infarcted myocardium. Nature 2001;410:701–5. [PubMed: 11287958]

19. Chen J, Li Y, Wang L, Lu M, Zhang X, Chopp M. Therapeutic benefit of intracerebral transplantation of bone marrow stromal cells after cerebral ischemia in rats. J Neurol Sci 2001;189:49–57. [PubMed: 11535233]
20. Wang L, Li Y, Gautam SC, Zhang ZG, Lu M, Chopp M. Ischemic cerebral tissue and MCP-1 enhance rat bone marrow stromal cell migration in interface culture. Experimental Hematology 2002;30:831–6. [PubMed: 12135683]
21. Aubin JE. Osteoprogenitor cell frequency in rat bone marrow stromal populations: role for heterotypic cell-cell interactions in osteoblast differentiation. J Cell Biochem J Cell Biochem 1999;72:396–410.
22. Lennon DP, Haynesworth SE, Young RG, Dennis JE, Caplan AI. A Chemically-Defined Medium Supports in-Vitro Proliferation and Maintains the Osteochondral Potential of Rat Marrow-Derived Mesenchymal Stem-Cells. Exp Cell Res Exp Cell Res 1995;219:211–22.
23. Claes L, Eckert-Hubner K, Augat P. The effect of mechanical stability on local vascularization and tissue differentiation in callus healing. J Orthop Res 2002;20:1099–105. [PubMed: 12382978]
24. Wallace AL, Draper ER, Strachan RK, McCarthy ID, Hughes SP. The vascular response to fracture micromovement. Clin Orthop Relat Res 1994:281–90. [PubMed: 8156689]
25. Rhinelander FW. Tibial blood supply in relation to fracture healing. Clin Orthop Relat Res 1974:34–81. [PubMed: 4609655]
26. Gardner MJ, van der Meulen MC, Demetrakopoulos D, Wright TM, Myers ER, Bostrom MP. In vivo cyclic axial compression affects bone healing in the mouse tibia. J Orthop Res 2006;24:1679–86. [PubMed: 16788988]
27. Case ND, Duty AO, Ratcliffe A, Muller R, Guldberg RE. Bone formation on tissue-engineered cartilage constructs in vivo: effects of chondrocyte viability and mechanical loading. Tissue Eng 2003;9:587–96. [PubMed: 13678438]
28. Lucas TS, Bab IA, Lian JB, Stein GS, Jazrawi L, Majeska RJ, ttar-Namdar M, Einhorn TA. Stimulation of systemic bone formation induced by experimental blood loss. Clin Orthop Relat Res 1997:267–75. [PubMed: 9224265]
29. Einhorn TA, Simon G, Devlin VJ, Warman J, Sidhu SP, Vigorita VJ. The osteogenic response to distant skeletal injury. J Bone Joint Surg Am 1990;72:1374–8. [PubMed: 2229116]
30. Zhang P, Sun Q, Turner CH, Yokota H. Knee loading accelerates bone healing in mice. J Bone Miner Res 2007;22:1979–87. [PubMed: 17696761]
31. Weiss S, Baumgart R, Jochum M, Strasburger CJ, Bidlingmaier M. Systemic regulation of distraction osteogenesis: a cascade of biochemical factors. J Bone Miner Res 2002;17:1280–9. [PubMed: 12096842]
32. Holbein O, Neidlinger-Wilke C, Suger G, Kinzl L, Claes L. Ilizarov callus distraction produces systemic bone cell mitogens. J Orthop Res 1995;13:629–38. [PubMed: 7674080]
33. Kaspar D, Neidlinger-Wilke C, Holbein O, Claes L, Ignatius A. Mitogens are increased in the systemic circulation during bone callus healing. J Orthop Res 2003;21:320–5. [PubMed: 12568965]
34. Hansen-Algenstaedt N, Algenstaedt P, Bottcher A, Joscheck C, Schwarzloh B, Schaefer C, Muller I, Koike C, Ruther W, Fink B. Bilaterally increased VEGF-levels in muscles during experimental unilateral callus distraction. J Orthop Res 2003;21:805–12. [PubMed: 12919867]
35. Zimmermann G, Henle P, Kusswetter M, Moghaddam A, Wentzensen A, Richter W, Weiss S. TGF-beta1 as a marker of delayed fracture healing. Bone Bone 2005;36:779–85.
36. Devine SM, Bartholomew AM, Mahmud N, Nelson M, Patil S, Hardy W, Sturgeon C, Hewett T, Chung T, Stock W, Sher D, Weissman S, Ferrer K, Mosca J, Deans R, Moseley A, Hoffman R. Mesenchymal stem cells are capable of homing to the bone marrow of non-human primates following systemic infusion. Exp Hematol 2001;29:244–55. [PubMed: 11166464]
37. Pereira RF, Halford KW, O'Hara MD, Leeper DB, Sokolov BP, Pollard MD, Bagasra O, Prockop DJ. Cultured adherent cells from marrow can serve as long-lasting precursor cells for bone, cartilage, and lung in irradiated mice. Proc Natl Acad Sci U S A 1995;92:4857–61. [PubMed: 7761413]

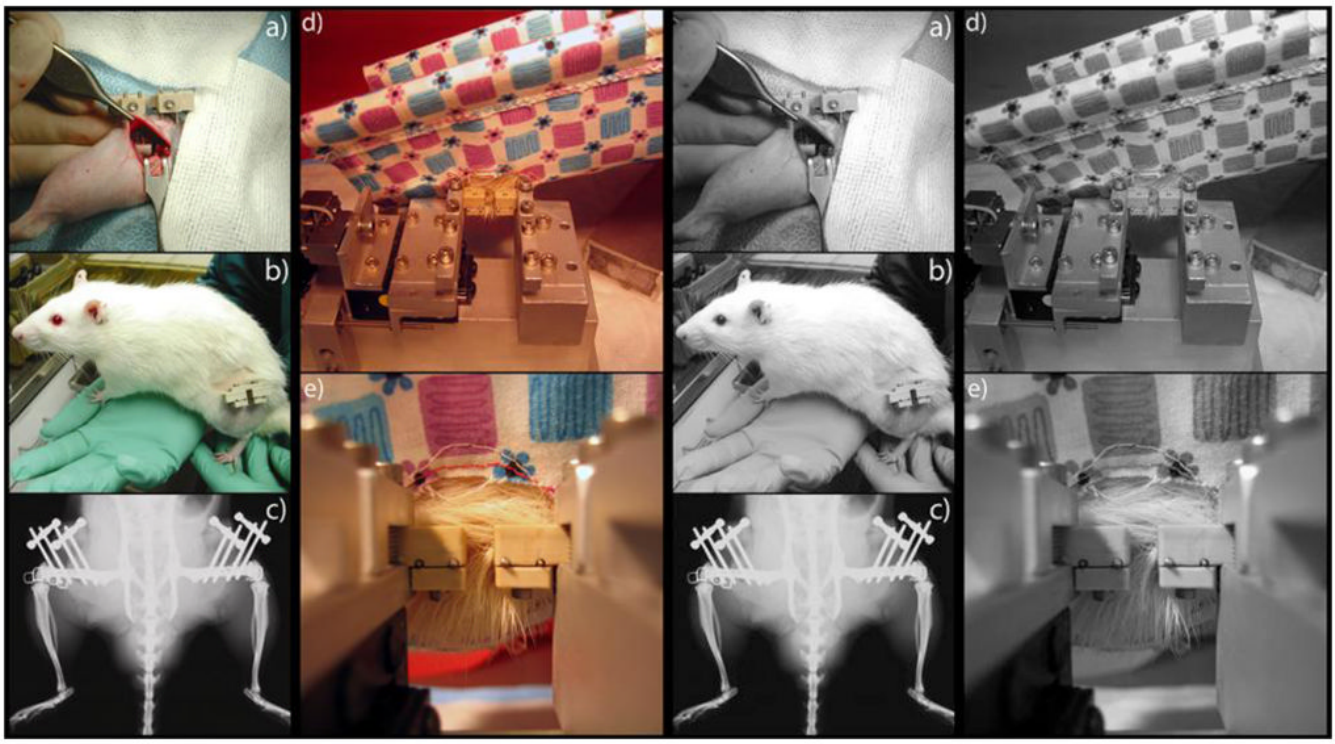

Figure 1. Overview of Surgery and Fixture for Axial Displacement

A two-millimeter segmental osteotomy was made at the mid-diaphysis of each femur (a). The fractures were stabilized using four threaded pins and a two-piece fixator that is locked in a rigid configuration for normal ambulation (b, c). During axial stimulation, the rat was anesthetized, placed in a sling, and the fixator was aligned with the fixture clamp (d). The close-up view of the fixator shows the two unlocked halves during stimulation (e).

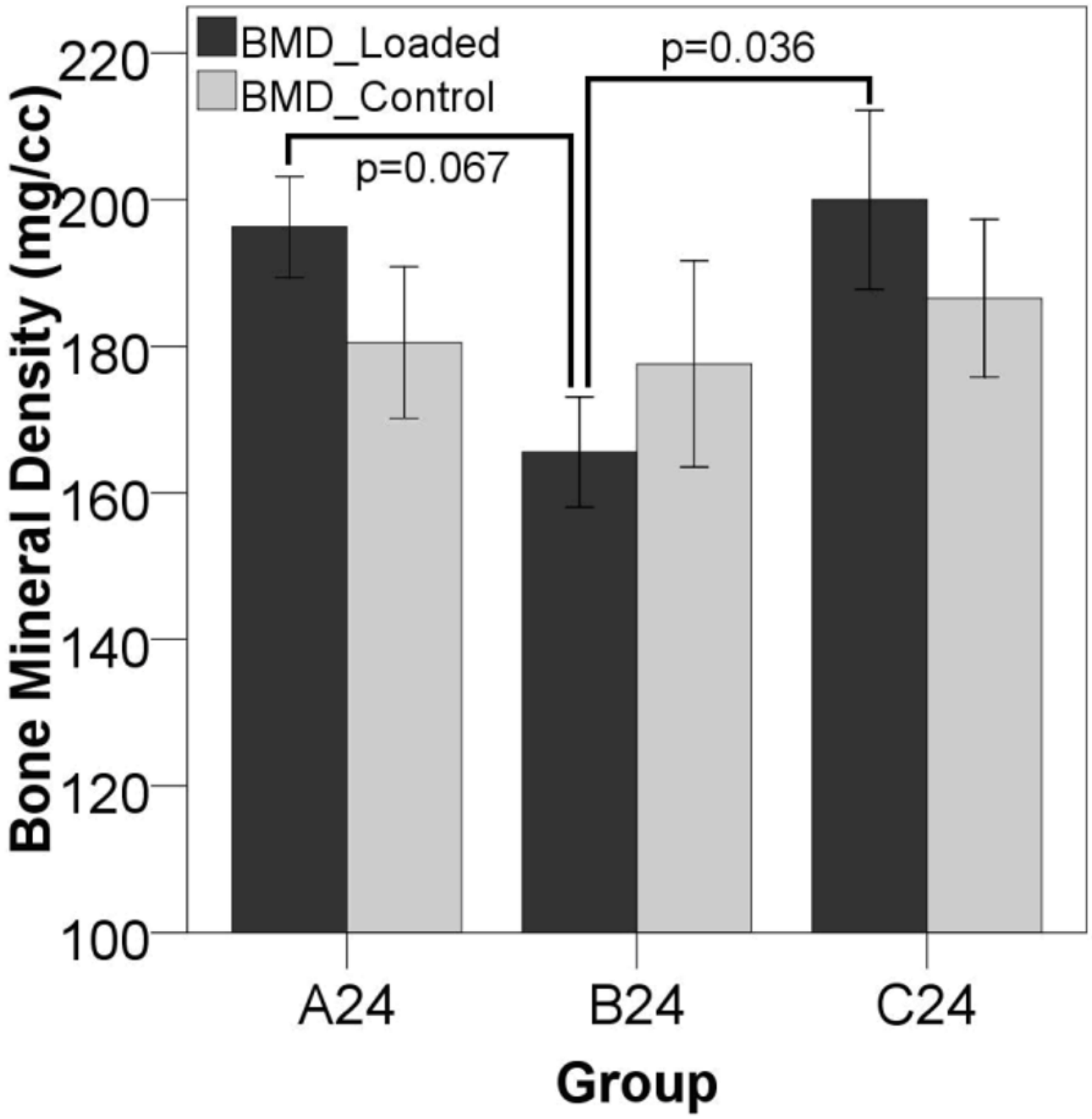

Figure 2. BMD 24 Days After Surgery

24 days after surgery, fractures stimulated at three days post-op (B24) have reduced BMD compared to to those displaced immediately after (A24) or ten days after surgery (C24) suggesting that mechanical stimulation during the inflammatory stage of healing leads to a subsequent reduction in callus mineralization.

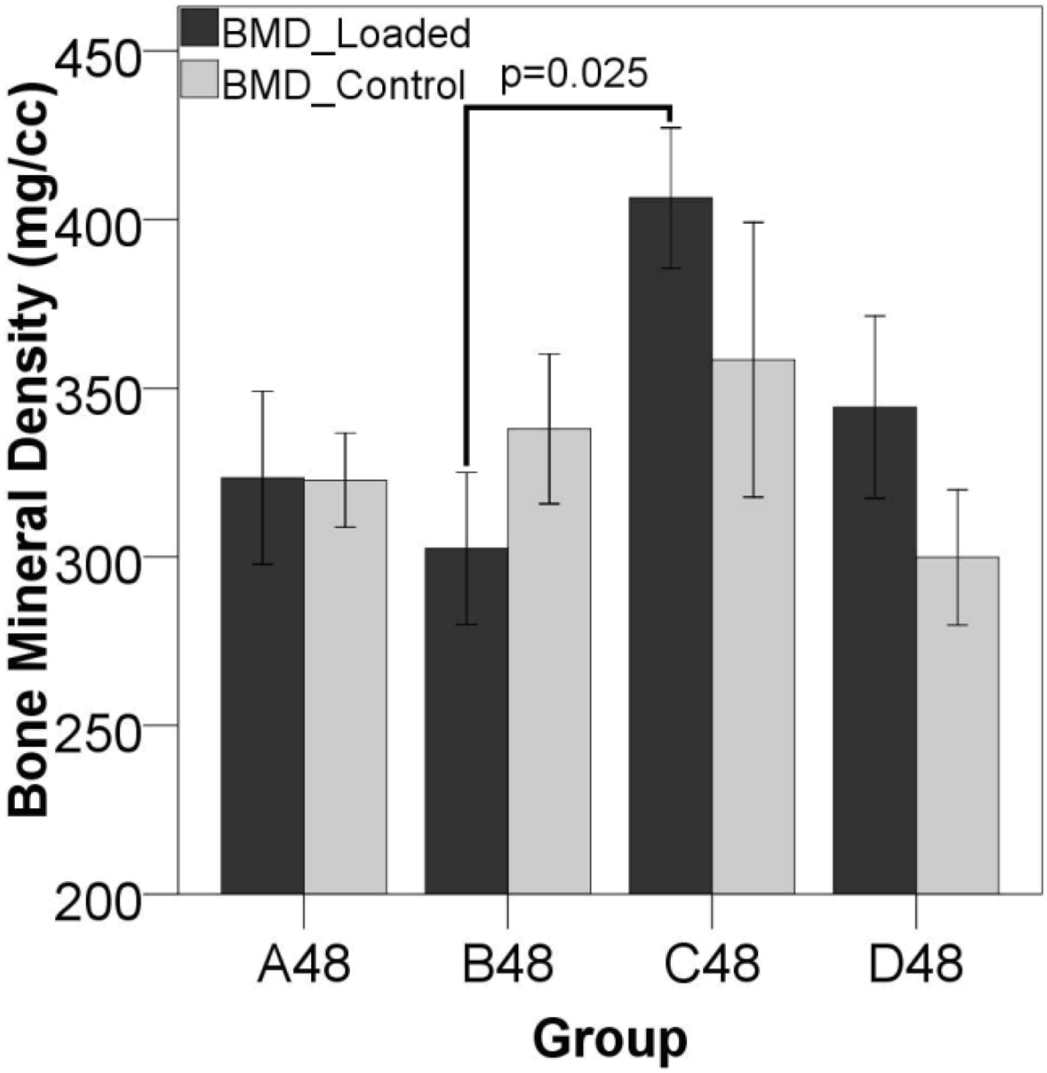

Figure 3. BMD 48 Days After Surgery

BMD is significantly higher in Group C (displacement beginning ten days post-op) versus Group B (displacement beginning three days post-op) 48 days after surgery. In the later stages of healing, the mineral content is higher on the displaced side in the animals loaded ten days post-operatively than those at other stimulation time points. This reached a significant increase over the defects displaced three days post-op, since the mineral levels in those gaps were slightly depressed compared to the other groups.

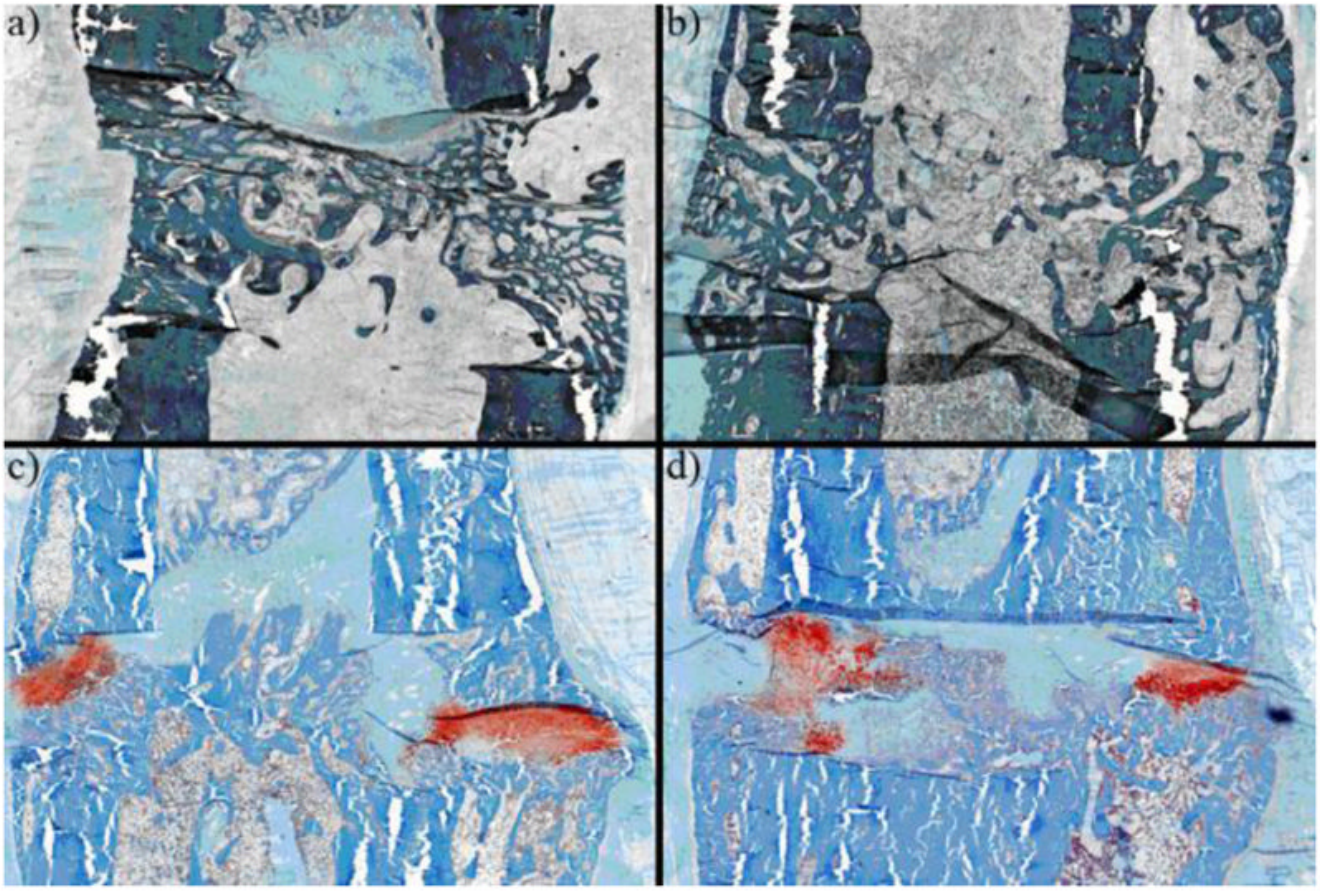

Figure 4. Histology for the Group Stimulated Ten Days After Surgery (Group C48)

When the axial displacement is started ten days after surgery, the stimulated limbs have no cartilage and have bony bridging by day 48 (shown above). The unstimulated controls have a substantial amount of bone, but still contain distinct areas of cartilage (in red). The figure shows: (a) a central section of a stimulated gap, (b) a peripheral section of a stimulated gap, (c) a central section of a control gap, and (d) a peripheral section of a control gap. Note that the difference in color between the top and the bottom images are an artifact of the staining procedure.

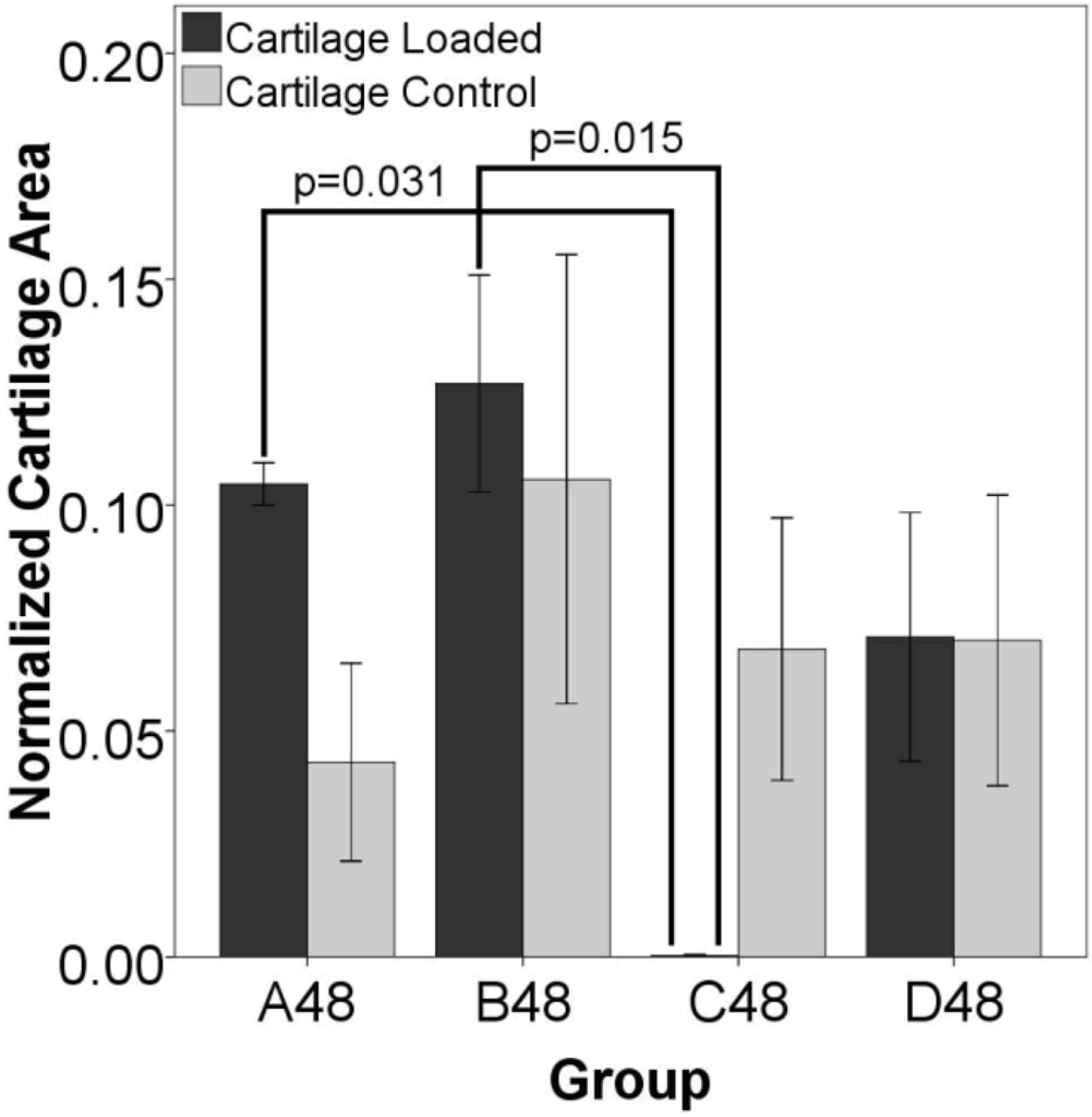

Figure 5. Cartilage area in animals euthanized 48 days post surgery

After 48 days, there is cartilage remaining in all groups, both stimulated and control, except for the gaps stimulated ten days after surgery (group C48). In these defects there is almost no cartilage remaining. The differences were significant between the displaced limbs of A48 and B48 in comparison to C48. There is also a significant difference between the displaced and contralateral control in group C48 (p=0.045, sig not shown), with the displaced side containing significantly less cartilage than the control. There is also more cartilage in the displaced side in group A48 when compared to the contralateral control (p=0.037, sig not shown).

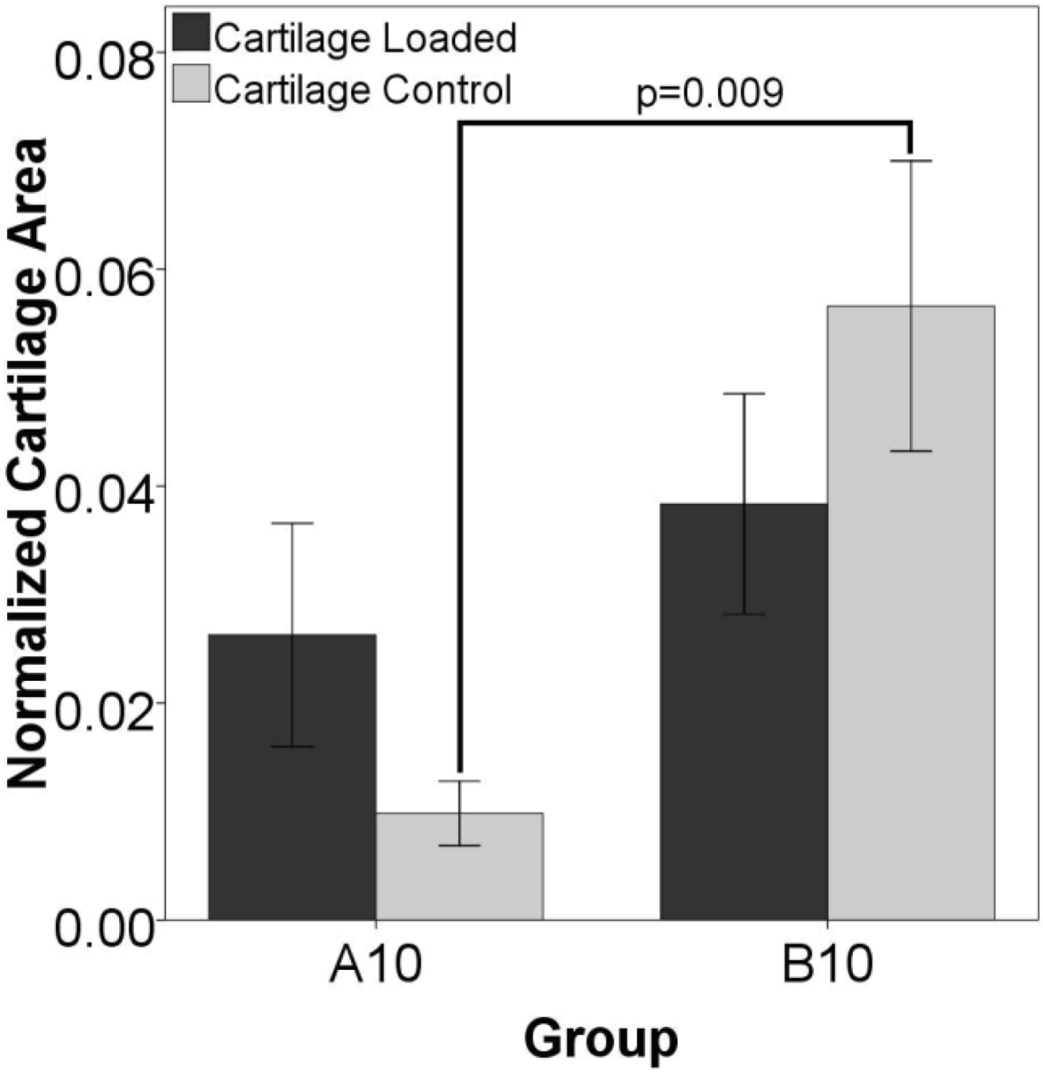

Figure 6. Histology Suggests a Systemic Effect

Histology shows differences between control limbs at day ten, suggesting a systemic effect. For animals euthanized ten days after surgery, there is an overall increase in cartilage area (stimulated and control combined) in the group stimulated three days after surgery (group B10) when compared to defects from animals stimulated immediately after surgery (group A10) (p=0.002). The control gaps from these animals also display an increased amount of cartilage (shown above), suggesting that there may be a systemic effect due to load.

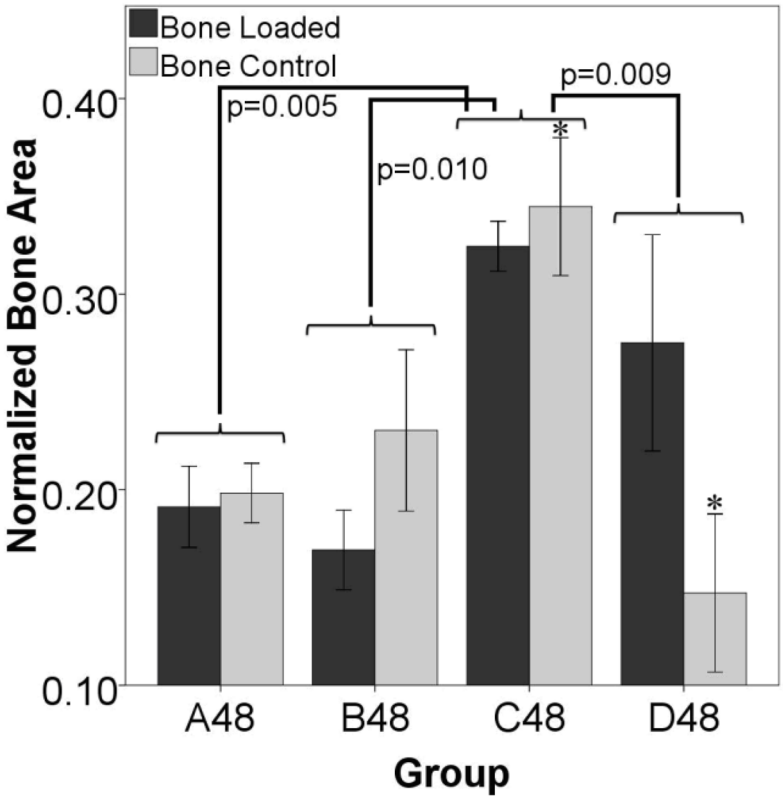

Figure 7. Bone Formation Suggests a Systemic Effect

Histology shows differences in normalized bone area from animals euthanized on day 48. The group loaded ten days after surgery (C48) has a higher percentage of bone as a whole (stimulated and control limbs considered together) than any other group (p=0.005 with group A, p=0.010 with group B, and p=0.009 with group D). There is also more bone in the control gap of C48 than in the control gap of D48 (*p=0.011). These results suggest that the applied stimulus is promoting more bone formation in both the loaded and control limbs in group C than for any other group.

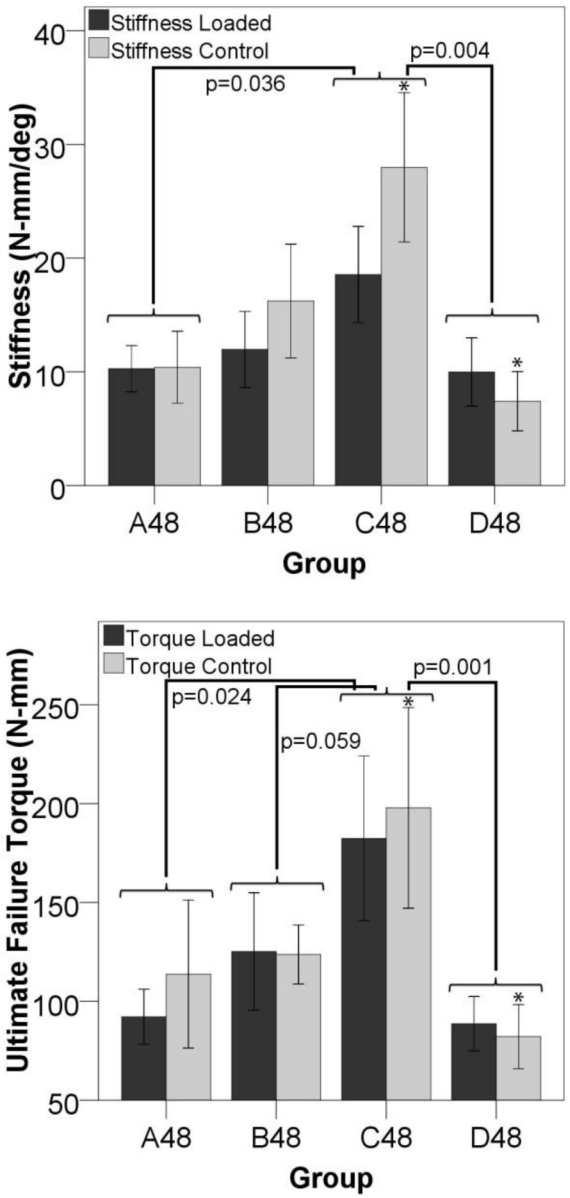

Figure 8. Mechanical Properties Suggest a Systemic Effect

The group loaded ten days after surgery (C48) is stiffer (p=0.036 versus group A and p=0.004 versus group D) and had a higher torque at failure (p=0.024 versus group A, p=0.059 versus group B, and p=0.001 versus group D) than any other group. The stiffness and ultimate failure torque are also higher in the control gaps of group C than in group D (*p<0.05). This suggests that the applied stimulus is promoting a more stiff and stronger structure in both the loaded and control limbs in group C than for any other group.

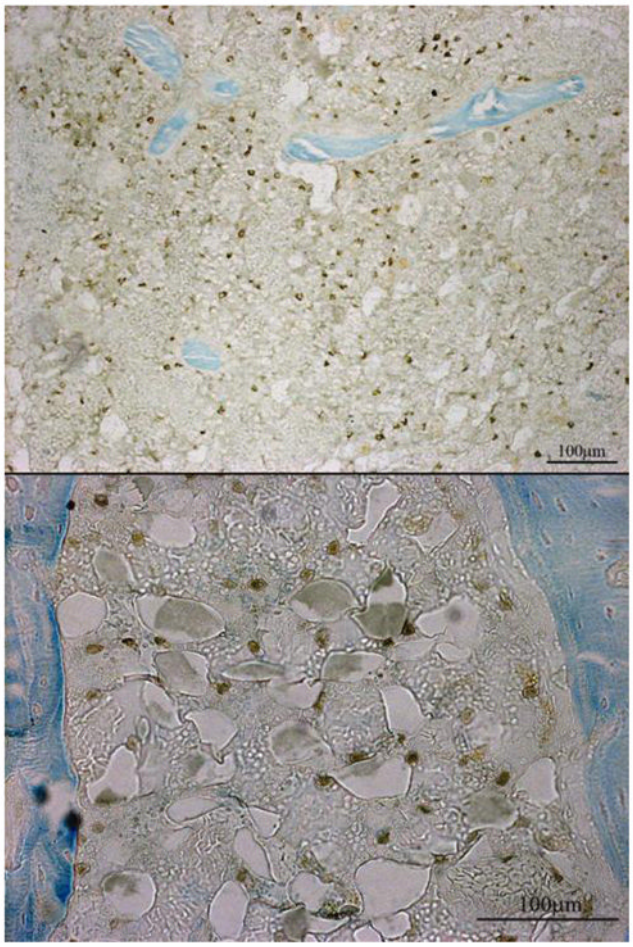

Figure 9. GFP Positive Cells in the Marrow

GFP positive cells were found in the marrow 48 days after surgery. At all of the time points there was evidence of some GFP positive staining, but it was not until day 48 that there were large populations of GFP positive cells in the marrow spaces. Group C48 showed evidence of a smaller population of GFP positive cells in comparison to the other groups euthanized on day 48 (A48, B48, and D48). Cells were also present in other locations (cortices and pin sites), but the most consistent location for the MSC populations was in the medullary marrow (top) and the marrow within the periosteal callus (bottom).

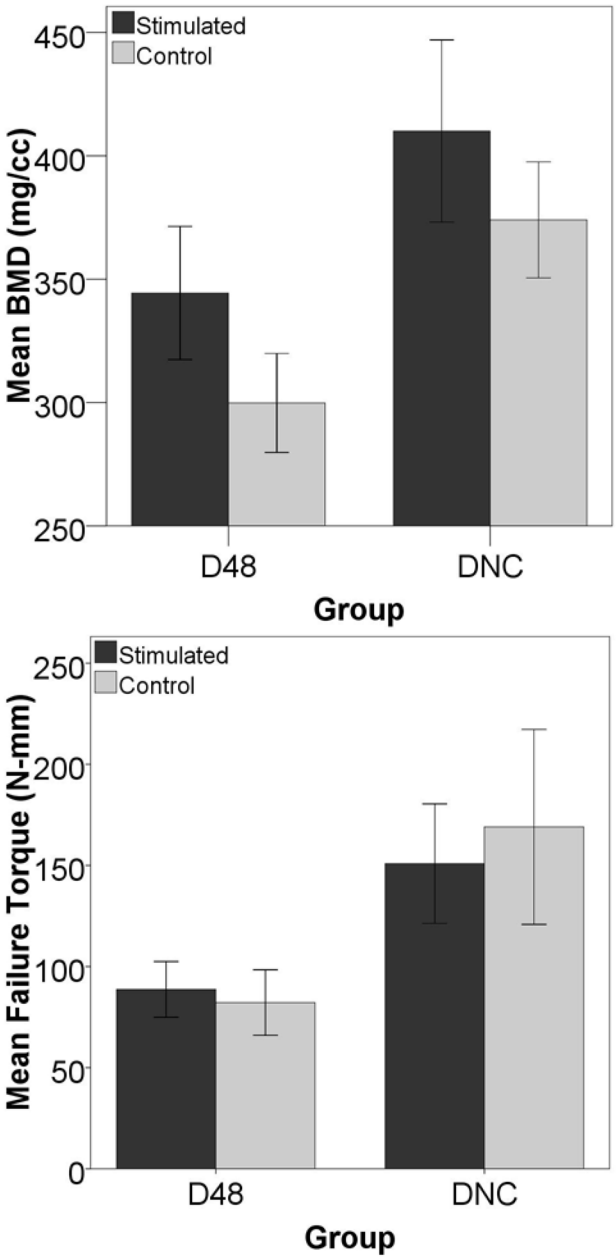

Figure 10. Cells produce an adverse effect as measured by micro-CT and mechanical testing in torsion

The group that was stimulated on day 24 but did not have exogenous cells introduced had a higher bone volume, represented above by BMD (p=0.011), than the group that had cells injected via the tail vein on day 24. The same decreases due to cell injection were seen in the stiffness of the callus in torsion (p=0.0301, data not shown) and the torque to failure (p=0.0142).

Table 1
Nomenclature and Expermiental Group Sizes

This table shows the nomenclature for each group used in the study. The letters correspond to the timing of mechanical stimulation, and the numbers correspond to the day of euthanasia. The numbers in parentheses show the number of animals that were entered into the study for micro-CT, histology, and torsion testing. All femora underwent micro-CT scanning, and the histology and torsion groups are subsets of that group.

Group	Displacement Initiation Day (Post-op)	Euthanasia Day 10: Group Name (µCT, histology, torsion)	Euthanasia Day 24: Group Name (µCT, histology, torsion)	Euthanasia Day 48: Group Name (µCT, histology, torsion)
A	0	A10 (n=11, 5, 5)	A24 (n=12, 3, 7)	A48 (n=8, 4, 4)
B	3	B10 (n=11, 5, 5)	B24 (n=11, 4, 5)	B48 (n=10, 3, 7)
C	10	--------	C24 (n=12, 5, 7)	C48 (n=11, 3, 5)
D	24	--------	--------	D48 (n=13, 5, 8)

Table 2
Amount of MSCs in the Marrow Spaces

The scores for the amount of MSCs in the marrow spaces of the displaced and control limbs for each group show the stimulated limbs have more cellular activity in the marrow when compared to the unstimulated control limbs. The number of cells also increases with the amount of time after injection (i.e. A48>A24>A10), except in group C, which had cell delivery and axial displacement begin ten days after surgery. The scoring system was developed due to difficulties in cell counting, and the scores represent three levels of cell populations: no cells, very few cells, and an established population of cells. A score of zero corresponds to no cells present, a score of one represents 1–10 cells, and a score of two signifies that 11 or more cells were present in the marrow.

Group	Marrow: Cell Score for Stimulated Limb	Marrow: Cell Score for Control Limb
A10	0.22	0.29
A24	0.52	0.50
A48	0.87	0.62
B10	0.13	0.11
B24	0.90	0.70
B48	1.38	1.04
C24	0.88	0.57
C48	0.67	0.42
D48	1.58	1.43